Validation of selfconsistent hybrid density functionals for the study of structural and electronic characteristics of organic π radicals

Carlo Adamo, Vincenzo Barone, and Alessandro Fortunelli

Articles you may be interested in

Solvation effects for polymers at an interface: A hybrid self-consistent field–density functional theory approach
J. Chem. Phys. 135, 204901 (2011); 10.1063/1.3662139

Structure of nonuniform fluid mixtures: A self-consistent density-functional approach
J. Chem. Phys. 117, 8933 (2002); 10.1063/1.1514650

Intrinsic bond strengths of multiple gallium–gallium bonds: A compliance matrix study using multiconfiguration self-consistent field wave functions and hybrid density functionals
J. Chem. Phys. 115, 6360 (2001); 10.1063/1.1377034

SelfConsistent Orbitals for Radicals
J. Chem. Phys. 22, 571 (1954); 10.1063/1.1740120

LCAO SelfConsistent Field Calculations of the πElectrons Energy Levels and Electronic Structure of Fulvene
J. Chem. Phys. 21, 953 (1953); 10.1063/1.1699088

Validation of self-consistent hybrid density functionals for the study of structural and electronic characteristics of organic π radicals

Carlo Adamo
Dipartimento di Chimica, Università della Basilicata via Nazario Sauro 85, I-85100 Potenza, Italy

Vincenzo Barone[a)]
Dipartimento di Chimica, Università Federico II, via Mezzocannone 4, I-80134 Napoli, Italy

Alessandro Fortunelli
Istituto di Chimica Quantistica ed Energetica Molecolare del CNR, via Risorgimento 35, I-56126 Pisa, Italy

Extensive density functional calculations are reported for the geometrical structures, thermochemistry, infrared, and hyperfine parameters of representative carbon-centered π radicals. Local functionals can be considered sufficient for geometrical and vibrational parameters, but seriously fail in the computation of thermochemical data and of spin-dependent properties. Gradient corrections (especially Becke exchange and Lee–Yang–Parr correlation functionals) sensibly improve matters. Inclusion of some Hartree–Fock exchange in a fully self-consistent density functional implementation delivers a further significant improvement, approaching the accuracy of the most refined post Hartree–Fock computations. Purposely tailored basis sets are also introduced which are small enough to be used in molecular computations, but still give high quality geometries and hyperfine coupling constants. © *1995 American Institute of Physics.*

I. INTRODUCTION

During the past few years, the structure of organic free radicals has been the object of increasing attention. Most of the investigations deal with the determination of the hyperfine splittings (hfs), in magnitude and sign, in relation to the geometry of the radical under consideration. Several experimental studies have provided a large amount of spectroscopic data, but interpretation of the results in structural terms is often difficult. This is particularly true in the field of free radicals due to the lack of precise structural determinations, and because spin properties often result from a delicate balance between different structural and electronic effects. These considerations have stimulated our interest toward the development of a well defined computational protocol ranging from the selection and testing of reliable electronic methods to the implementation of refined large amplitude Hamiltonians to describe vibrational averaging effects from large amplitude nuclear motions. While the dynamical treatment developed by one of us in a number of studies (e.g., Ref. 1) can easily be applied to large systems characterized by a limited number of large amplitude vibrations, extension of electronic computations is less straightforward. In fact, the hyperfine splittings derived from electron paramagnetic resonance (EPR) spectra can be factored into an isotropic part (Fermi contact term), and an anisotropic (dipolar) part. Because of the global nature of the corresponding operator, predictions of anisotropic coupling constants are often reliable already at the Hartree–Fock (HF) level, provided that adequate basis sets are used. The situation is much more involved for isotropic terms, which are extremely sensitive to basis set, correlation, and geometry.[1–3] This has stimulated much work, and the most sophisticated post Hartree–Fock

(especially coupled cluster[4–7] or multireference configuration interaction[7–9]) models are providing wave functions of sufficient quality. This class of methods is, however, too expensive for systematic studies of large molecules. In such circumstances other theoretical approaches deserve particular attention. The merits of the density functional (DF) theory, by far the most useful nonempirical alternative to conventional post Hartree–Fock methods for studying physicochemical properties of molecules, are currently well recognized.[10–13] Gradient-corrected functionals have significantly increased the reliability of DF methods, and recent work has shown that small modifications of the functional form[13] or partial inclusion of the Hartree–Fock exchange[14,15] can provide even better results. Concerning more specifically hyperfine splittings, only qualitative trends have been reproduced in a number of studies with the unrestricted Kohn–Sham (UKS) formalism in the framework of the local spin density (LSD) approximation.[16] Much improved results have been recently obtained by at least three different groups[17–22] introducing gradient corrections in the approximate exchange-correlation functionals. These studies showed, however, a strong dependence of the results on the molecular geometry and on the choice of the auxiliary basis sets used to fit Coulomb, exchange, and correlation potentials, not to speak about the convergence of the results with the dimensions of the orbital basis set. Furthermore, huge modifications are often induced by different contraction patterns of the orbital basis sets. As a consequence, it is difficult to ascertain if the discrepancies with experimental data are due to the inadequacies of the orbital and/or auxiliary basis set or to inadequacies of the theoretical models that have been used. An analysis of these effects has been recently performed by one of us for atoms and diatomic molecules using very large basis sets and integration grids with a program which avoids the use of auxiliary basis sets.[23,24] Together with local and

---

[a)]Author to whom all correspondence should be addressed.

gradient corrected functionals, hybrid functionals including some Hartree–Fock exchange have been considered. The original implementation of these hybrid functionals[14,15] would be useless in the present context, since HF exchange is added only at the end of the iterative SCF procedure, i.e., to a wave function obtained in the local spin density approximation. Furthermore experimental geometries are used for molecular systems. The fully consistent approach adopted in our studies involves, instead, the use of the complete density functional (including gradient corrections and some Hartree–Fock exchange) in each stage of the SCF process and (for molecular systems) during geometry optimization. The results of these studies suggested that a particular hybrid functional (B3LYP, *vide infra*) coupled with a relatively small purposely built basis set could provide the heart of a standard protocol (functional, basis set, etc.) for the study of structure-property characteristics of organic free radicals, which can be used with confidence also by nonspecialists, as an interpretational aid to experimental determinations. In the present paper we will validate this protocol by performing a number of computations for representative carbon-centered π radicals, which probably represent the class of free radicals for which more extensive experimental and theoretical data are available. Furthermore, the number of different structural situations encountered in this class of radicals provides a very severe benchmark for our approach. As a reference system we have chosen the methyl radical, which will be treated with a number of basis sets and density functionals. Next, other systems will be treated only by the B3LYP self-consistent hybrid functional, and by two medium size basis sets.

In closing this section we point out that our approach is fully consistent in that one-electron properties are computed using structures optimized by the same method and, when needed, vibrational averaging is performed in terms of vibrational modes obtained in the same way. Furthermore, the class of radicals selected in the present study is particularly demanding since, contrary to standard post Hartree–Fock procedures, π radicals are more demanding than σ ones for methods based on density functional theory.[20]

II. THE METHOD

All computations have been performed within the UKS formalism using the Gaussian 92/DFT system of programs.[25] Among the characteristics of this code we mention the use of Gaussian basis functions, the avoidance of auxiliary functions, the implementation of *pruned* grids, and the availability of analytical first and second derivatives.[12,26–28] On the basis of some test computations with very large grids, the standard SG-1 grid[26] has been selected for the present study. The stability of the UKS single determinant wave function with respect to complex variations, symmetry breaking, etc. has been always checked. Local spin density (LSD) computations have been carried out using the exchange energy of the uniform electron gas[29] (UEG) and the Vosko, Wilk, and Nusair (VWN) correlation[30] functional. Gradient corrections have been introduced using the Becke exchange part (B) (Ref. 31) and either the Perdew (P86) (Ref. 32) or the Lee–Yang Parr (LYP) (Ref. 32) correlation parts. In standard no-

menclature, the former method is sometimes referred to as BP86, and the latter as BLYP. Note that the VWN contribution is not included when using the LYP correlation potential. The original Becke's three-parameter functional[15] (hereafter referred to as B3PW91) has the form

$$E^{\text{B3PW91}} = E_{xc}^{\text{LSD}} + (1 - a_0)(E_x^{\text{exact}} - E_X^{\text{UEG}}) + a_X \Delta E_x^B + a_c \Delta E_c^{\text{PW91}}. \tag{1}$$

The Perdew–Wang gradient correction to the correlation functional (ΔE_C^{PW91}) [Ref. 32(b)] can be replaced by P86 or LYP functionals leading to B3P86 and B3LYP models, respectively. Our choice of the B3LYP form is based on the particularly good performances of the BLYP parent functional in thermochemical problems[12,13] and on some limits of the PW91 (Ref. 21) and P86 (Ref. 23) functionals for EPR parameters. Since the LYP functional contains both a local part and a gradient correction, only the latter contribution should be used to obtain a coherent implementation. However, it has been recently shown that the local part of the LYP functional is very similar to the VWN parametrization of the correlation energy in the free electron gas.[34] As a consequence, we approximate the last term in Eq. (1) by

$$\Delta E_C \approx E_C^{\text{LYP}} - E_C^{\text{VWN}}. \tag{2}$$

A number of tests showed that values of the three semiempirical coefficients appearing in Eq. (1) near 0.80 provide the best results, irrespective of the particular form of the different functionals. We will use here the values ($a_0 = 0.80$, $a_X = 0.72$, and $a_C = 0.81$) determined by Becke from a best fitting of the heats of formation of a standard set of molecules.[15]

The formulas for calculating hyperfine parameters are obtained from the spin Hamiltonian,

$$H_{\text{spin}} = -g_e \beta_e S_z B_z - g_N \beta_N I_z B_z + S \cdot T \cdot I. \tag{3}$$

The first two contributions are the electronic and nuclear Zeeman terms, respectively, and arise from the interactions between a magnetic field **B** and the magnetic moments of the unpaired electrons (S_z) or the magnetic nuclei (I_z) in the system. The remainder is the hyperfine interaction term, and is a result of the interactions between the unpaired electrons and the nuclei. β_e, β_N are the electron and nuclear magnetons, and g_e, g_N the electron and nuclear magnetogyric ratios.

The 3×3 hyperfine interaction tensor T can be further separated into its isotropic (spherically symmetric) and anisotropic (dipolar) components. Isotropic hyperfine splittings $A_{\text{iso}}^{(N)}$ are related to the spin densities $\rho^s(r_N)$ at the corresponding nuclei by

$$A_{\text{iso}}^{(N)} = \frac{8\pi}{3} \frac{g_e}{g_0} g_N \beta_N \sum_{\mu,\nu} P_{\mu,\nu}^{\alpha-\beta} \langle \varphi_\mu | \delta(r_{kN}) | \varphi_\nu \rangle. \tag{4}$$

Computation of these terms is straightforward and is already included in most *ab initio* codes.

The anisotropic components are derived from the classical expression of interacting dipoles:

TABLE I. Orbital exponents and contraction coefficients of the DZP′ basis set.

	Carbon		Oxygen		Hydrogen	
	Orbital exponent	Contr. coefficient	Orbital exponent	Contr. coefficient	Orbital exponent	Contr. coefficient
s orbitals	4232.61	0.002 03	7816.54	0.002 03	127.950	0.010 74
	634.882	0.015 54	1175.82	0.015 44	19.2406	0.119 54
	146.097	0.075 41	273.188	0.073 77	2.8992	0.926 42
	42.4974	0.257 12	81.1696	0.247 61	0.6534	1.0
	14.1892	0.596 56	27.1836	0.611 83	0.1776	1.0
	5.1477	1.0	9.5322	1.0		
	1.9666	1.0	3.4136	1.0		
	0.4962	1.0	0.9398	1.0		
	0.1533	1.0	0.2846	1.0		
p orbitals	18.1557	0.018 53	35.1832	0.019 58	0.727	1.0
	3.9864	0.115 44	7.9040	0.124 19		
	1.1429	0.386 21	2.3051	0.394 73		
	0.3594	0.640 09	0.7171	0.627 38		
	0.1146	1.0	0.2137	1.0		
d orbitals	0.550	1.0	1.185	1.0		

$$A_{i,j}^{(N)} = \frac{g_e}{g_0} g_N \beta_N \sum_{\mu,\nu} P_{\mu,\nu}^{\alpha-\beta}$$

$$\times \langle \varphi_\mu | r_{kN}^{-5}(r_{kN}^2 \delta_{i,j} - 3 r_{kN,i} r_{k,N,j}) | \varphi_\nu \rangle. \qquad (5)$$

These terms are more complicated to compute, and also to determine experimentally. They are, however, strictly related to field-gradient integrals already available in several standard *ab initio* packages. For linear molecules, the molecular symmetry axis is chosen as one of the components say Z. Since the tensor is traceless, there remains only one meaningful diagonal element, say T_{ZZ} with $T_{ZZ}=-2T_{XX}=-2T_{YY}$. The quantity A_{dip}, defined by $A_{\text{dip}}=\frac{1}{2}T_{ZZ}$ is called the dipolar hyperfine coupling constant. Frosch and Foley introduced a different set of parameters a, b, c, and d to describe the hyperfine interaction in diatomic molecules.[35] These parameters, preferred by microwave (MW) spectroscopists, are related to A_{iso} and A_{dip} as $A_{\text{iso}}=b+c/3$ and $A_{\text{dip}}=c/3$. In the present paper we will treat the isotropic and the anisotropic hyperfine coupling constants separately.

The hfs are usually given in units of MHz by MW spectroscopist, and in Gauss or mT (1 G=0.1 mT) by EPR spectroscopists. In the present work all the theoretical hfs are given in MHz; to convert data to gauss one has to divide by $2.8025 g_e/g_0$, where g_0 is the g factor of the electron in individual radicals.

A very large basis set must be next selected for reference purposes. For second row atoms this has been obtained by coupling the $18s,13p$ basis set recently optimized by Partridge[36] to the $4d,3f$ polarization set used by Roos and co-workers in the development of density averaged atomic natural orbitals.[37] The basis set for hydrogen has been obtained adding to the $8s$ set of Ref. 38, two tight s functions (ζ=17 907,2683), one diffuse s function (ζ=0.027 962), and the $4p$ polarization set of Ref. 37. The basis set (hereafter referred to as EXT) is left completely uncontracted in all the computations. This basis set is, of course, too large to be routinely used in molecular computations. It is, therefore,

important to build a manageable basis set able to deliver sufficiently reliable geometries and spectroscopic constants. Previous experience with post Hartree–Fock methods[1,39] suggests that the Huzinaga (9,5) primitive set[40] provides a good starting point. According to some recent work,[11,13] converged geometries and thermodynamic quantities are obtained from DF methods starting from triple ζ basis sets augmented by double sets of polarization functions. At this level, different primitive sets and contraction patterns are essentially equivalent. On the other hand, computation of reliable spin-dependent properties requires the addition of diffuse valence functions and decontraction of the outer core, inner valence part of the s functions.[1,39] Although computation of reliable multipolar moments and polarizabilities also requires the inclusion of a set of diffuse polarization functions,[23,24,41] this enhancement has not been considered in the present study. Both polarization and diffuse functions are taken from the correlation consistent sets recently developed by Dunning.[42] In the case of hydrogen, two tight functions (ζ =533.124, 88.854) have been added to the $4s$ Huzinaga set[40] and only the three innermost primitive functions have been contracted. As usual, a scale factor of 1.2 has been next introduced for molecular computations.[43] Taking into account all the aforementioned considerations we expect that the resulting $(10,6,2;6,2)/[6,4,2;4,2]$ basis set (hereafter referred to as TZ2P′) would perform quite well. The contraction coefficients of this basis set have been, next, optimized in atomic UKS computations. We have also tested a smaller basis set which does not include diffuse functions, has a single set of polarization functions, and uses a 2ζ contraction of valence p orbitals. This basis set will be referred to as DZP′ (see Table I).

The reliability of the DF approach has been checked, when experimental data are not available, with reference to unrestricted Hartree–Fock (UHF), quadratic configurations interaction with single and double replacements (UQCISD), and multiconfigurational self-consistent (MCSCF) computa-
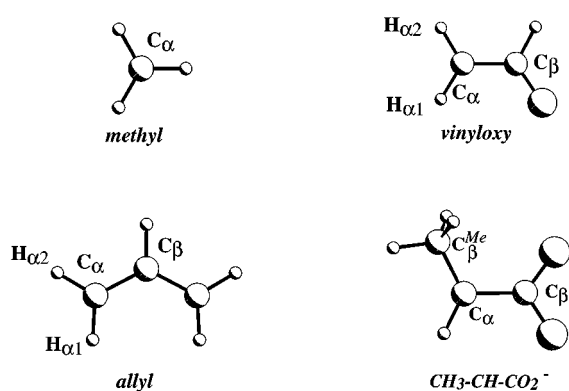
FIG. 1. Structure and atom labeling for carbon-centered π radicals for which some experimental data are available.

FIG. 2. Structure and atom labeling of Schiff base radicals.

tions. Together with the basis sets described, we have employed also the standard polarized 6-31G(d,p) (Ref. 44) and 6-311G(d,p) (Ref. 45) basis sets. Some computations have been also performed using a split valence contraction[46] of the Huzinaga (9,5) primitive set[40] without any polarization function (hereafter referred to as DZ for coherence with previous work[19]). All the *ab initio* computations have been performed with the GAUSSIAN 92/DFT code, too.

III. RESULTS AND DISCUSSION

The whole series of radicals studied in the present work is shown in Figs. 1 and 2. Together with methyl (used as a model for studying basis set effects) we have considered a number of conjugated π radicals which, together with their intrinsic interest, have the advantage of being fairly rigid species for which vibrational averaging effects can be probably neglected. The hfs of some of the radicals (allyl, $CH_3CHCO_2^-$, vinyloxy, see Fig. 1) are experimentally well characterized, thus providing a valid benchmark. Further comparisons are possible with the structures and vibrational frequencies available either from experiment or from refined post Hartree–Fock computations. Schiff base radicals (Fig. 2) have been, instead, only recently characterized and only in association with transition metal ions.[47] It was, therefore, interesting to investigate intrinsic structures and magnetic properties of these species without the perturbing effect of a coordinated metal atom. The more so as some theoretical computations of *hfs* are available.[19]

In order to discuss the phenomenology of *hfs*, the hydrogen and carbon atoms will be labeled according to the relative position with respect to the formal radical center $H_\alpha, H_\beta, H_\gamma, C_\alpha, C_\beta, C_\gamma$. Furthermore, the H_β atoms will be further distinguished into two groups, whether they lie in the symmetry plane of a conjugated system, or they belong to a methyl group attached to the radical center (see Figs. 1 and 2).

A. CH$_3$ as a benchmark

The methyl radical has been chosen as a benchmark for different density functionals and basis sets. From an experimental point of view, the structure,[48] atomization energy,[12]
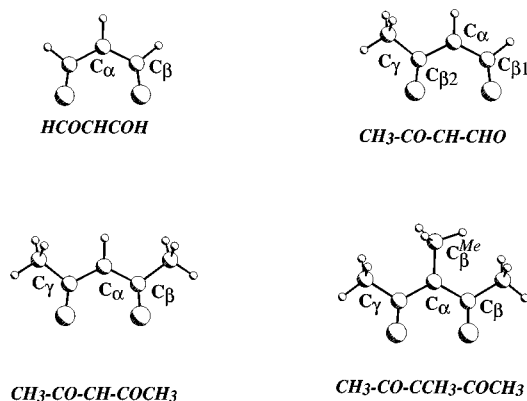
vibrational frequencies,[48] and EPR parameters[49–53] of this radical are well characterized. Moreover, the theoretical literature is very rich.[1,54–58] The results are shown in Table II. It is apparent that, while the isotropic hyperfine coupling of hydrogen is approximately constant with all the functionals used, the splitting of carbon is strongly dependent on the functional form. In particular, the local spin density approximation appears insufficient, and also the results obtained when gradient corrections are introduced by Becke (exchange) and Perdew (correlation) functionals are not satisfactory. Better results are obtained when correlation is treated by the LYP functional. Table II shows that the results are further improved coupling a combination of Becke and Hartree–Fock exchange to the LYP correlation functional (B3LYP model). At this level the results are competitive with the most sophisticated (and much more expensive) post Hartree–Fock procedures. We have also computed the effect of vibrational averaging on the hyperfine structure of CH$_3$ by the procedure described in detail in Ref. 1. The results reported in Table II confirm that the effect is particularly significant for the carbon atom and point out the reliability of DF methods also in this connection.

The effect of gradient corrections on total and spin electron densities has been previously investigated by Ziegler and co-workers.[59,60] They found that the main difference relative to LSD is a removal of density from the core and valence tail regions, and an increase of the core density. Direct contribution to isotropic hyperfine couplings are well reproduced at this level, as confirmed by the very good results obtained for σ radicals,[17,18] where this term is dominant. On the other hand the isotropic hyperfine couplings of π radicals are dominated by spin polarization effects, which are somewhat underestimated by standard density functionals. Addition of some Hartree–Fock exchange then slightly increases this contribution, leading to good agreement with experiment. Within the standard delta function formulation, the Fermi contact term depends only on the local quality of the wave function at the nuclei. The fact that Gaussian functions do not satisfy the correct cusp condition at the nuclei could impair the computation of this kind of properties. Our results show that this problem can be overcome by using

TABLE II. Selected properties of the methyl radical obtained by different functionals and basis sets (see text for details).

Parameter[a]	B3LYP EXT	B3LYP DZP′	B3LYP TZ2P′	LSD TZ2P′	BP86 TZ2P′	BLYP TZ2P′	Expt.
CH	1.077	1.083	1.079	1.088	1.087	1.085	1.079[b]
De	310.7	307.7	310.8	342.9	318.2	322.6	307.4[c]
S^2	0.754	0.753	0.754	0.752	0.754	0.753	0.750
$A_{iso}C$	89.9	84.9	83.4	30.5	64.5	76.3	
$A_{iso}H$	−64.8	−63.1	−65.4	−50.7	−64.0	−60.8	
$A_{dip}C$	81.3	74.3	77.1	75.4	76.9	77.9	63[d],61[e]
$A_{dip}H$	40.3,1.7	40.1,0.9	40.1,0.2	38.6,0.4	39.2,0.5	39.3,0.1	35,1.4[f]
$\langle A_{iso}C \rangle$	117.7	112.6	111.1	58.2	92.2	104.0	107.3[g]
$\langle A_{iso}H \rangle$	−59.2	−57.5	−59.8	−45.1	−58.4	−55.2	−64.7[g]

[a]Bond length in Å, atomization energy (De) in kcal mol^{-1}, expectation value of spin squared, and hyperfine couplings in MHz. For isotropic hyperfine couplings, both equilibrium (planar) and vibrationally averaged ($\langle \rangle$) values are given.
[b]Reference 48.
[c]Reference 12.
[d]Reference 50.
[e]Reference 51.
[f]Reference 52.
[g]Reference 49.

sufficiently large basis sets (e.g., EXT) or, more effectively, by adding to standard basis sets very tight s functions (e.g., DZP′ or TZ2P′).

Anisotropic coupling constants are much less sensitive to the functional form, and essentially converged results are obtained already within the local spin density approximation. The results of Table II show that all the DFT results are in semiquantitative agreement with the reference data. This is particularly significant since anisotropic coupling constants are much harder to obtain experimentally, and since DF methods can handle much larger molecules than conventional post Hartree–Fock methods.

One of the motivations for the introduction of self-consistent hybrid functionals is the hope to obtain with the same method and basis set good structures, thermochemical, and spectroscopic properties. This is particularly significant for open shell species for which experimental structures are often not available. The results of Table II show that the geometry and atomization energy obtained by the B3LYP/TZ2P′ model are in close agreement with experiment. XH bond lengths are slightly overestimated, but this general tendency of DF approaches[12,13,18] is strongly reduced by the B3LYP functional. What is even more promising is the remarkable agreement between TZ2P′ and EXT basis sets for all the properties considered. For the computation of EPR parameters also the cheaper DZP′ basis set appears suf-

ficient. On these grounds we will discuss in the following sections only B3LYP/DZP′ and B3LYP/TZ2P′ results.

As a last point we recall that since hfs are quantities very sensitive to all sort of effects, care should be used in checking the convergence of the iterative process. From such a viewpoint, we found the GAUSSIAN92/DFT results more stable against changes in molecular orientation, etc., than those of DeMon.[19] However, there still remain minor discrepancies between the present calculations and those reported in Ref. 20: we were not able to obtain the same results with the BP86 functional even using a fully saturated Gaussian basis set (the EXT one). This might be due to the different implementation of the DF procedures in the two sets of codes.

B. Conjugated radicals

In previous work[19] we have shown that reasonable geometries can be obtained for nonconjugated systems at quite low computational levels. We found, in particular, that only negligible modifications of hfs are obtained in going from UHF/DZ geometries to the best available ones. Coming to conjugated radicals we concentrate our attention on two representative systems, namely allyl (CH_2CHCH_2) and the prototype of Schiff base radicals (HCOCHCOH).

The allyl radical has been investigated by many experimental techniques, including photodetachment,[61] EPR,[49,62]

TABLE III. Geometry (Å and degrees) of the allyl radical according to different methods (see text for details).

	UHF DZ	UHF 6-31G(d,p)	UHF DZP′	UHF TZ2P′	UMP2 6-31G(d,p)	CAS MIDI3*[a]	B3LYP DZP′	B3LYP TZ2P′
$C_\alpha C_\beta$	1.404	1.390	1.398	1.386	1.377	1.388	1.396	1.381
$C_\beta H_\beta$	1.076	1.079	1.080	1.077	1.088	1.087	1.089	1.085
$C_\alpha H_\alpha 1$	1.075	1.076	1.078	1.074	1.084	1.084	1.086	1.082
$C_\alpha H_\alpha 2$	1.074	1.074	1.077	1.073	1.082	1.082	1.085	1.080
$C_\alpha C_\beta H_\beta$	117.70	117.73	117.81	117.73	117.81	117.52	117.51	117.48
$H_\alpha 1 C_\alpha C_\beta$	121.28	121.14	121.07	121.09	121.03	121.21	121.06	121.06
$H_\alpha 2 C_\alpha C_\beta$	121.27	121.34	121.16	121.26	121.77	121.38	121.42	121.42

[a]From Ref. 87.

TABLE IV. Calculated harmonic wave numbers (cm^{-1}) and (in parenthesis) IR intensities (in $km\,mol^{-1}$) for the allyl radical C_3H_5 (C_{2v}).

Symmetry	Mode	Description	UHF/6-31G(d)[a]	UMP2/6-31G(d)[a]	MR-ACPF/MIDI3*[b]	B3LYP/DZP′	B3LYP/TZ2P′	Expt.
				In-plane				
	ν_1	asym CH_2 stretch	3422	3333	3146(39.4)	3254(15.1)	3245(15.6)	3107 (m)[c]
	ν_2	sym CH_2 stretch	3325	3222	3066 (2.0)	3155 (1.3)	3151 (4.4)	3051 (w)[c]
	ν_3	CH stretch	3336	3246	3045 (2.2)	3149(12.9)	3139(11.9)	3019 (m)[c]
$A1$	ν_4	CH_2 scissoring	1647	1595	1491 (3.0)	1524 (4.5)	1519 (1.6)	1488 (m)[d]
	ν_5	CC str., CH_2 rock	1341	1301	1269 (0.9)	1267 (0.4)	1275 (1.1)	1245 (w)[d]
	ν_6	CH_2 rock, CC str.	1075	1048	1035 (0.3)	1031 (0.3)	1040 (0.1)	1068(vw)[d]
	ν_7	CCC bending	451	437	418 (0.0)	429 (0.1)	436 (0.1)	427[d]
	ν_8	asym CH_2 stretch	3418	3329	3142 (5.1)	3251 (3.0)	3242 (4.4)	3107(w)[c,e]
	ν_9	sym CH_2 stretch	3324	3238	3055 (2.5)	3146 (5.3)	3145 (7.2)	3019 (m)[c]
$B2$	ν_{10}	CH_2 sc., CH rock CC str.	1637	1579	1498 (0.0)	1517 (2.0)	1526 (3.1)	1463 (m)[d]
	ν_{11}	CH rock, CH_2 scissoring	1537	1444	1400 (8.3)	1418 (6.2)	1433 (5.4)	1389 (m)[c]
	ν_{12}	CC stretch	1251	1230	1206 (0.3)	1203 (0.7)	1208 (0.7)	1184 (w)[c]
	ν_{13}	CH_2 rock	1005	918	913 (0.3)	937 (0.3)	945 (0.1)	/
				Out-of-plane				
	ν_{14}	CH_2 wagging	780	801	738 (0.0)	779 (0.0)	792 (0.0)	/
$A2$	ν_{15}	CH_2 twisting	572	595	547 (0.0)	544 (0.0)	549 (0.0)	549[d]
	ν_{16}	CH wag, CH_2 twist	1035	1123	986(22.3)	996(19.6)	1008(20.9)	983 (m)[c]
$B1$	ν_{17}	CH_2 wagging	799	823	751(64.4)	802(96.8)	815(80.0)	802 (vs)[c]
	ν_{18}	CH_2 twist, CH wag	547	557	524(14.6)	526(16.3)	529(18.2)	518[d]

[a] Reference 83.
[b] Reference 87.
[c] IR data from Ref. 69.
[d] RRS data from Refs. 77 and 79.
[e] Shoulder.

absorption,[63–66] matrix IR,[67–70] multiphoton ionization,[71–74] gas-phase high resolution IR,[75,76] and resonance raman spectroscopy (RRS).[77–81] The geometry and vibrational structure of the ground electronic state have been examined in a number of theoretical calculations.[82–88] According to Takada and Dupuis[82] and Szalay *et al.*[87] a 3 π orbital/3 electron MCSCF wave function—hereafter referred to as CAS(3,3)—is suitable for the determination of the structure and vibrational frequencies of the allyl radical. We therefore repeated this type of computation using the DZP′ basis set, which is essentially of double ζ quality, and thus analogous to the MIDI3* basis set used in Ref. 87. As one can see from Table III there is a striking similarity between the resulting CAS(3,3) and B3LYP geometries, the major difference being obtained for the C_α–C_β bond length, which comes out a bit longer from the B3LYP method. However, further inclusion of correlation effects,[87] increases the C_α–C_β bond distance to 1.395 Å, in close agreement with the B3LYP result. There are also minor differences in the CH bond lengths, which are slightly longer in the B3LYP method.

The computed vibrational frequencies of allyl radical are shown in Table IV. Our assignment of normal modes is in complete agreement with those of Szalay *et al.*[87] and Cometta-Morini *et al.*[84] The correct number of vibrational modes for C_{2v} symmetry were identified: $7a_1+6b_2+3b_1+2a_2$. From a quantitative point of view, our unscaled frequencies are competitive with those obtained by the most sophisticated post Hartree–Fock methods. Furthermore, the error is essentially constant for all kinds of normal modes except those dominated by CH stretchings for which anharmonicity is particularly significant. It is also noteworthy that the results obtained by DZP′ and TZ2P′ basis sets are very similar. This confirms that DFT methods are much less demanding than conventional correlated approaches in terms of basis set saturation.

In analogy with the allyl radical, for the Schiff base radical HCOCHCOH we performed *ab initio* geometry optimizations with a 5 π orbital/5 electron CAS wave function. The resulting geometrical parameters are given in Table V: it is clear on inspection that the major differences reside in the

TABLE V. Geometry (Å and degrees) of HCOCHCOH ($^2B_1$ state) according to different methods (see text for details).

	UHF DZ	UHF 6-31G(d,p)	UHF DZP′	UHF TZ2P′	CAS DZP′	B3LYP DZP′	B3LYP TZ2P′	B3LYP DZP′[a]
$C_\alpha C_\beta$	1.431	1.443	1.451	1.445	1.467	1.467	1.455	1.410
$C_\beta O$	1.285	1.223	1.223	1.212	1.216	1.228	1.218	1.258
$C_\beta H_\beta$	1.079	1.089	1.091	1.089	1.092	1.109	1.106	1.102
$C_\alpha H_\alpha$	1.074	1.077	1.079	1.075	1.078	1.090	1.085	1.081
$C_\alpha C_\beta O$	124.85	124.66	124.86	124.98	124.99	125.35	125.31	122.62
$C_\alpha C_\beta H_\beta$	117.05	115.70	115.41	115.29	114.99	113.98	114.30	124.57
$H_\alpha C_\alpha C_\beta$	115.83	116.62	116.44	116.33	116.68	116.57	116.43	116.57

[a] $^2B_2$ state.

TABLE VI. Isotropic hyperfine coupling constants (MHz) for H_2CCHCH_2 obtained by different methods (see the text for details).

Geometry Wave function	UHF/DZ B3LYP/DZP′	UHF/DZP′ B3LYP/DZP′	CAS/MIDI3* B3LYP/DZP′	B3LYP/DZP′ B3LYP/DZP′	B3LYP/TZ2P′ B3LYP/TZ2P′	Expt.[a]
$A_{iso}(H_\alpha 1)$	−39.3	−39.4	−39.3	−39.5	−40.7	−39.0
$A_{iso}(H_\alpha 2)$	−41.4	−41.4	−41.5	−41.7	−43.4	−41.5
$A_{iso}(H_\beta)$	12.3	12.2	12.1	12.2	12.4	11.8
$A_{iso}(C_\alpha)$	55.4	55.0	54.9	55.8	53.5	61.4
$A_{iso}(C_\beta)$	−50.2	−49.7	−49.2	−50.0	−47.8	−48.2

[a]References 49 and 62.

CO and CH bond lengths, which are slightly overestimated by the DF optimization. Note, at variance with the case of allyl, the extreme sensitivity of CC and CO distances to basis set extension: at the UHF level, e.g., the CO bond length is reduced by ≈ 0.06 Å in passing from the DZ to the DZP′ basis set. By admitting that—as is usually the case—further correlation effects increase the *ab initio* CO bond length and produce a value closer to the B3LYP one, we conclude that the main difference resides in the CH bond lengths, which are slightly overestimated by the B3LYP procedure. Since this does not occur in hydrocarbon radicals, we guess that this is due to the presence of electronegative atoms (the oxygens), which hinder a uniform description of the molecular correlation energy. We stress, however, that the results would have been uniformly worse without the contemporary inclusion of gradient corrections and some Hartree–Fock exchange in the density functional: the LSD approximation is known to poorly describe the CH bond, and even the inclusion of gradient corrections does not assure completely satisfactory results. Previous studies[89,90] have shown that partial inclusion of Hartree–Fock exchange in the DF improves also CO bond lengths.

On the whole, we conclude that the B3LYP geometries are approximately as accurate as the best available *ab initio* ones, provided that the same basis set is used in the two approaches. From Tables III and V it is clear that, as previously noted,[91] the UHF method also furnishes results not too distant from the DF or CAS ones. Only the CH bond lengths of the allyl radical and the CC bond distance in HCOCH-COH are somewhat underestimated by the UHF approach. However, this difference is sufficient to produce significant variations of hfs with respect to the CAS or B3LYP geometries for Schiff base radicals (see the following). It is also noteworthy that the results obtained by the DZP′ basis set are not fully converged neither at the *ab initio*, nor at the B3LYP level; in particular, all the bond distances slightly shrink in passing to the TZ2P′ basis set (which is, instead,

essentially converged at the B3LYP level, giving geometries very close to those obtained with the EXT basis set). However, we will see later that the DZP′ basis set is able to deliver reasonably accurate hfs values at a computational cost which is sensibly lower than that of the TZ2P′ one, thus allowing one to investigate medium to large size radicals.

Let us now analyze how the geometrical parameters affect the hfs values for conjugated radicals. For the allyl radical there are, as shown in Table VI, minor variations of the hfs values with the method chosen for optimizing the geometry: with double ζ+polarization basis sets these variations are not larger than 2% for all kind of atoms. A more appreciable variation is found, instead, in passing from the DZP′ to the TZ2P′ basis set, amounting to 5% in the worst case: values at the H atoms tend to increase, whereas hfs of C atoms tend to decrease. Note, however, that the B3LYP/DZP′ values at the B3LYP/DZP′ geometry are generally in better agreement with experiment than B3LYP/TZ2P′ values at B3LYP/TZ2P′ geometry, thus providing a reasonable compromise between accuracy and computational cost. One has essentially the same overall accuracy which is obtained through the best available post HF methods, but with a sensibly smaller computational cost. Note also that the agreement with experiment at the α carbon atom of the allyl radical would probably be improved through proper inclusion of vibrational averaging effects.

A more complex situation is found with the HCOCH-COH radical (see Table VII). First of all, the large difference between the DZ and DZP′ geometries (see Table V) is reflected in the large variations of the hfs values in passing from UHF/DZ to, e.g., B3LYP/DZP′ geometries. Note, however, that the results are much more homogeneous when comparing geometries obtained utilizing different methodologies, but the same (DZP′) basis set: the variations here are about 2% for H_α atoms, 35% for H_β atoms (this is not particularly meaningful due to the negligible value of the hfs at that atoms), 6% for C_α atoms, and 3% for C_β atoms. Finally,

TABLE VII. Isotropic hyperfine coupling constants (MHz) for HCOCHCOH ($^2B_1$ state) obtained by different methods (see text for details).

Geometry Wave function	UHF/DZ B3LYP/DZP′	UHF/6-31G(d,p) B3LYP/DZP′	UHF/DZP′ B3LYP/DZP′	CAS/DZP′ B3LYP/DZP′	B3LYP/DZP′ B3LYP/DZP′	B3LYP/TZ2P′ B3LYP/TZ2P′	B3LYP/DZP′[a] B3LYP/DZP′
$A_{iso}(H_\alpha)$	−39.6	−43.8	−44.2	−45.3	−45.2	−47.5	−7.6
$A_{iso}(H_\beta)$	5.1	1.5	1.3	0.8	1.0	1.1	145.2
$A_{iso}(C_\alpha)$	52.9	58.2	60.0	63.4	63.8	61.1	−17.0
$A_{iso}(C_\beta)$	−42.1	−37.0	−37.0	−36.3	−37.5	−36.1	−33.8

[a] $^2B_2$ state.

TABLE VIII. Geometrical parameters (Å and degrees) obtained by CAS(5,3)/DZP′ or B3LYP/DZP′ computations for the vinyloxy radical. At these geometries hyperfine splittings (in MHz) are obtained by UQCISD/DZ or B3LYP/DZP computations. The labeling of atoms is given in Fig. 1.

Parameter		CAS	B3LYP
$C_\alpha H_{\alpha_1}$		1.076	1.086
$C_\alpha H_{\alpha_2}$		1.076	1.086
$C_\alpha C_\beta$		1.445	1.435
$C_\beta O$		1.225	1.243
$C_\beta H_\beta$		1.091	1.106
$H_{\alpha_1} C_\alpha C_\beta$		119.51	119.47
$H_{\alpha_1} C_\alpha C_\beta$		120.81	121.16
$C_\alpha C_\beta O$		122.75	123.07
$H_\beta C_\beta C_\alpha$		117.45	116.47
UQCISD	$A_{iso}(H_{\alpha_1})$	82.9(53.4)[a]	81.1(52.2)
	$A_{iso}(H_{\alpha_2})$	83.5(53.8)[a]	82.1(52.8)
B3LYP	$A_{iso}(H_{\alpha_1})$	50.1	49.1
	$A_{iso}(H_{\alpha_2})$	50.6	50.0

[a]Extrapolated (see text) values are given in parentheses.

in passing to the TZ2P′ basis set one observes the usual increase of the hfs at the H atoms and the usual decrease at the C atoms, slightly more pronounced for H_α atoms than in the case of allyl. On the whole, one can say that the B3LYP/DZP′ method reasonably describes these radicals, even though the uncertainty in the description seems to be larger for the Schiff base one. The true problem, however, is that the predicted hfs values for the H atoms of HCOCH-COH do not agree with the extrapolated UQCISD values of Ref. 92: At the UHF/DZ geometry one has a H_α value of −39.6 MHz vs an extrapolated *ab initio* value of −44.2 MHz, while at the UHF/6-31G(d,p) geometry one has a H_α value of −43.8 MHz vs an extrapolated *ab initio* value of −47.7 MHz. The trend is essentially the same in the two approaches, but the B3LYP absolute values are significantly smaller. Furthermore, the *ab initio* results were confirmed in Ref. 19 by extrapolated values obtained using the Perdew–Wang functional for exchange (Ref. 93) and the Perdew functional for correlation[32] (PWP calculations). Since there

are no experimental data on the isolated ligands, there still remains the open question of which approach is more reliable. A possible answer to this problem can be given by the study of the vinyloxy radical (see Fig. 1), which can be thought as a simplified prototype of the Schiff base radicals, and for which there exist experimental data for hfs at H_α atoms.[94] The results of geometry optimizations at the CAS(3,5)/DZP′ (we have chosen a 3,5 rather than a 3,3 optimization as in Ref. 95) and B3LYP/DZP′ levels, and hfs computations using the B3LYP/DZP′ and UQCISD/DZ approaches (at the optimized geometries) are given in Table VIII. One immediately notes the close similarity of the two sets of values: Even though the CO and CH bond lengths come out slightly larger from the B3LYP approach, the computed hfs values differ at the two geometries by at most 1 MHz. Although we do not report the values for the other atoms it is noteworthy that the analogous difference is 0.8 Mhz for H_β and C_α values, whereas it increases to $\approx$1.7 MHz for the C_β atom. One thus gets from B3LYP/DZP′ computations an average value for hfs at H_α atoms of −49.6 or −50.4 MHZ using B3LYP or CAS(3,5) optimized geometries, respectively. On the other hand, the corresponding UQCISD (extrapolated) values read −52.6 and −53.6 MHz. The extrapolation factor 0.644 has been taken from Ref. 92; the use of the same factor at different geometries (but with the same basis set) is justified, since there are only minor modifications in passing from *ab initio* to B3LYP geometries. Analogously, PWP calculations of the type described in Ref. 19 give −51.6 and −53.0 MHz. Both UQCISD/DZ and PWP/DZP′ extrapolated values are thus slightly closer to the experimental average of −55.6 MHz than the B3LYP values. Our final conclusion is thus that the B3LYP approach might underestimate the hfs values of H_α atoms in the Schiff base radicals by 3–6 MHz.

As a final remark we note that for HCOCHCOH there exist two states of different symmetry very close in energy, the ΔE between $^2B_1$ and $^2B_2$ states being just 1.5 kcal mol^{-1} at the B3LYP/DZP′ level. As shown in Tables V and VII, the geometries and hfs are significantly different for the two

TABLE IX. Geometries (Å and degrees) of methylated Schiff base radicals obtained by CAS/DZP′ and B3LYP/DZP′ computations (see the text for details). The π skeleton is always planar and, unless otherwise specified, the three hydrogen atoms of methyl groups are symmetrically disposed with respect to the fourth carbon bond with fixed tetrahedral angles (109.4712°).

	$CH_3COCHCHO$			$CH_3COCHCOCH_3$			$CH_3COCCH_3COCH_3$	
Parameter	CAS	B3LYP	Parameter	CAS	B3LYP	Parameter	CAS	B3LYP
$C_\alpha H_\alpha$	1.078	1.090						
$C_\alpha C_{\beta_1}$	1.480	1.482						
$C_\alpha C_{\beta_2}$	1.464	1.463				$C_\alpha C_\beta^{Me}$	1.520	1.516
$C_{\beta_1} O$	1.216	1.229	$C_\alpha H_\alpha$	1.078	1.090	$C_\alpha C_\beta$	1.492	1.494
$C_{\beta_2} O$	1.214	1.227	$C_\gamma H_\gamma$	1.086	1.094	$C_\beta^{Me} H_\beta$	1.083	1.093
$C_{\beta_1} H_\beta$	1.092	1.109	$C_\alpha C_\beta$	1.479	1.479	$C_\gamma H_\gamma$	1.085	1.093
$C_\gamma H_\gamma$	1.086	1.094	$C_\beta C_\gamma$	1.519	1.531	$C_\beta C_\gamma$	1.525	1.535
$C_{\beta_2} C_\gamma$	1.519	1.529	$C_b O$	1.215	1.229	$C_\beta O$	1.215	1.228
$H_\alpha C_\alpha C_{\beta_1}$	116.01	115.93	$H_\alpha C_\alpha C_\beta$	116.63	116.60	$C_\beta^{Me} C_\alpha C_\beta$	119.41	119.41
$H_\alpha C_\alpha C_{\beta_2}$	117.25	117.23	$C_\alpha C_\beta C_\gamma$	115.94	115.33	$C_\alpha C_\beta C_\gamma$	118.61	117.79
$C_\alpha C_{\beta_1} O$	125.46	125.90	$C_\alpha C_\beta O$	122.65	122.88	$C_\alpha C_\beta O$	122.21	122.58
$C_\alpha C_{\beta_2} O$	122.19	122.31						
$C_\alpha C_{\beta_2} C_\gamma$	116.13	115.56						
$H_\beta C_{\beta_1} C_\alpha$	114.76	113.71						

TABLE X. Isotropic hyperfine splittings of methylated Schiff base radicals obtained by B3LYP/DZP′ computations at CAS/DZP′ or B3LYP/DZP′ geometries (see the text for details).

CH$_3$COCHCHO			CH$_3$COCHCOCH$_3$			CH$_3$COCCH$_3$COCH$_3$		
Atom	CAS	B3LYP	Atom	CAS	B3LYP	Atom	CAS	B3LYP
H$_\alpha$	−46.4	−46.2				H$_\beta$	56.0	56.7
H$_\beta$	0.4	0.8	H$_\alpha$	−47.6	−47.5	H$_\gamma$	−3.2	−3.4
H$_\gamma$	−2.5	−2.8	H$_\gamma$	−2.3	−2.6	C$_\alpha$	72.8	72.2
C$_\alpha$	65.7	66.1	C$_\alpha$	68.7	68.9	C$_\beta^{Me}$	−23.0	−23.4
C$_{\beta_1}$	37.5	38.9	C$_\beta$	−35.1	−36.2	C$_\beta$	−34.1	−34.9
C$_{\beta_2}$	−33.8	−34.7	C$_\gamma$	−1.7	−1.5	C$_\gamma$	−2.2	−2.1
C$_\gamma$	−1.6	−1.4						

electronic states. As a matter of fact, the $^2B_2$ state corresponds to a σ radical with the consequent very large hfs at H$_\beta$. However, when one adds a Na$^+$ atom to the system to mimic the presence of a transition metal ion [e.g., Co(III) as in Ref. 47] the $^2B_1$ state is strongly stabilized (we were actually not able to converge our calculations on the $^2B_2$ state) so that it should be the only state detected in EPR spectra of metal complexes. In this connection it is noteworthy that the hfs computed in the presence of the Na$^+$ ion do not differ by more than 3 MHz from those obtained for the insulated radical, and that they tend to increase, as realized in the experimental situation.[47]

The changes of geometrical parameters and hyperfine splittings induced by progressive replacement of hydrogen atoms by methyl groups in the Schiff base radicals are shown in Tables IX and X, respectively. Geometries were optimized at the CAS(5,5)/DZP′ and B3LYP/DZP′ levels, whereas hfs were evaluated by the B3LYP/DZP′ approach using both sets of geometries. From an analysis of these results one can derive the following points. (a) The overall appearance is very close to the results on the simplest Schiff base (the HCOCHCOH radical) reported in Tables V and VII (see also the analogous results on the vinyloxy radical shown in Table VII): the CC bond distances and the valence angles are very similar by the two methods, whereas the CO and CH bond distances come out slightly larger from B3LYP computations. (b) Despite these differences, the hfs obtained by B3LYP/DZP′ computations at the two different geometries are practically coincident: the average discrepancy is generally smaller than 0.4 MHz, with the exception of the C$_\beta$ atoms, for which it can be as large as 1.3 MHz. (c) The progressive substitution of hydrogen atoms by methyl groups generally tends to increase the hfs at H$_\alpha$ and C$_\alpha$ atoms, and to decrease the hfs at C$_\beta$ atoms: this trend is in agreement with experimental results (also quantitatively).[47]

One of the methyl groups in the CH$_3$COC(CH$_3$)COCH$_3$ radical is bound to a conjugated system. To investigate whether the B3LYP approach is able to correctly predict the hfs at H$_\beta^{Me}$ atoms, we have checked its performances on a radical derived from alanine (the radical CH$_3$CHCO$_2^-$, see Fig. 1) for which hfs at hydrogen atoms have been experimentally determined.[96] The B3LYP/DZP′ results are −55.7 MHz for the H$_\alpha$ atom and 64.8 MHz for the average of H$_\beta^{Me}$ atoms. Both values are close to the experimental values of −53.8 and 70.1 MHz, respectively. The problems encoun-tered in previous work[19] with the hfs at H$_\beta^{Me}$ atoms were thus probably due to the poor geometry obtained at the UHF/DZ level.

IV. CONCLUSION

We have performed density functional calculations on representative π radicals, and have found that the method performs remarkably well. Introduction of gradient corrections and some Hartree–Fock exchange in a fully consistent density functional approach provides structures, harmonic force fields, and thermochemical data of nearly chemical accuracy. Furthermore the computed hyperfine couplings approach the values obtained by the most sophisticated post Hartree–Fock methods for both H and C atoms. Taking into account previous tests on other molecular systems, it can be concluded that hybrid methods like B3LYP couple the advantages of local (good geometries) and gradient corrected (good one-electron properties and energetic quantities) functionals with an improved overall accuracy.

Contrary to methods based on an Hartree–Fock zero-order wave function, DF approaches appear equally reliable for closed and open shell systems. Furthermore, the speed of the computations and the availability of analytical first and second derivatives offer the opportunity of characterizing complete potential energy surfaces. Although further work is needed concerning the transferability of these trends to other systems, the first results suggest that self consistent hybrid density functionals with purposely tailored basis sets provide a promising theoretical tool for the study of structural and spectroscopic characteristics of large organic free radicals.

[1] V. Barone, C. Minichino, A. Grand, and R. Subra, J. Chem. Phys. **99**, 6787 (1993).
[2] I. Carmichael, Chem. Phys. **116**, 351 (1987).
[3] D. Feller and E. R. Davidson, in *Theoretical models of Chemical Bonding, Part 3*, edited by Z. B. Maksic (Springer, Berlin, 1991).
[4] R. J. Bartlett and H. Sekino, J. Chem. Phys. **82**, 4225 (1985).
[5] I. Carmichael J. Chem. Phys. **91**, 1072 (1989).
[6] S. A. Perera, J. D. Watts, and R. J. Bartlett, J. Chem. Phys. **100**, 1425 (1994).

[7] D. Feller, E. Glendening, and E. A. McCullough, Jr., J. Symons J. Chem. Phys. **99**, 2829 (1993).

[8] D. Feller and E. R. Davidson, J. Chem. Phys. **88**, 7580 (1988).

[9] B. Fernandez, P. Jørgensen, E. A. McCullough, Jr., and J. Symons, J. Chem. Phys. **99**, 5995 (1993).

[10] J. Andzelm and E. Wimmer, J. Chem. Phys. **96**, 1280 (1992).

[11] T. Ziegler, Chem. Rev. **91**, 651 (1991).

[12] B. G. Johnson, P. M. W. Gill, and J. A. Pople, J. Chem. Phys. **98**, 5612 (1993).

[13] G. J. Laming, V. Termath, and N. C. Handy, J. Chem. Phys. **99**, 8765 (1993).

[14] A. D. Becke, J. Chem. Phys. **98**, 1372 (1993).

[15] A. D. Becke, J. Chem. Phys. **98**, 5648 (1993).

[16] H. Akai, M. Akai, S. Blügel, B. Drittler, H. Ebert, K. Terakura, R. Zeller, and P. H. Dederichs, Prog. Theor. Phys. Suppl. **101**, 11 (1990).

[17] V. Barone, C. Adamo, and N. Russo, Chem. Phys. Lett. **212**, 5 (1993).

[18] V. Barone, C. Adamo, and N. Russo, Int. J. Quantum Chem. (to be published).

[19] C. Adamo, V. Barone, and A. Fortunelli, J. Phys. Chem. **98**, 8648 (1994).

[20] N. Ishii and T. Shimizu, Phys. Rev. A **48**, 1691 (1993); Chem. Phys. Lett **225**, 462 (1994).

[21] L. A. Eriksson, V. G. Malkin, O. L. Malkina, and D. R. Salahub, J. Chem. Phys. **99**, 9756 (1993); **100**, 5066 (1994).

[22] J. Kong, L. A. Eriksson, and R. J. Boyd, Chem. Phys. Lett. **217**, 24 (1994).

[23] V. Barone, J. Chem. Phys. **101**, 6834 (1994).

[24] V. Barone, Chem. Phys. Lett. **226**, 392 (1994).

[25] M. J. Frisch, G. W. Trucks, M. Head-Gordon, P. M. W. Gill, M. W. Wong, J. B. Foresman, B. G. Johnson, H. B. Schlegel, M. A. Robb, E. S. Replogle, R. Gomperts, J. L. Andres, K. Raghavachari, J. S. Binkley, C. Gonzalez, R. L. Martin, D. J. Fox, D. J. DeFrees, J. Baker, J. J. P. Stewart, and J. A. Pople, GAUSSIAN92/DFT, Gaussian Inc., Pittsburgh, P. A. (1993).

[26] P. M. W. Gill, B. G. Johnson, and J. A. Pople, Chem. Phys. Lett. **209**, 506 (1993).

[27] B. G. Johnson and M. J. Frisch, Chem. Phys. Lett. **216**, 133 (1993).

[28] B. G. Johnson and M. J. Frisch, J. Chem. Phys. **100**, 7429 (1994).

[29] P. A. M. Dirac, Proc. Cambridge Philos. Soc. **26**, 376 (1930).

[30] S. H. Vosko, L. Wilk, and M. Nusair, Can. J. Phys. **58**, 1200 (1980).

[31] A. D. Becke, Phys. Rev. B **38**, 3098 (1988).

[32] (a) J. P. Perdew, Phys. Rev. B **33**, 8822 (1986); (b) J. P. Perdew, in *Electronic Structure of Solids*, edited by P. Ziesche and H. Eschrig (Akademie Verlag, Berlin, 1991); J. P. Perdew, J. A. Chevary, S. H. Vosko, K. A. Jackson, M. R. Pederson, D. J. Singh, and C. Fiolhais, Phys. Rev. B **46**, 6671 (1992).

[33] C. Lee, W. Yang, and R. G. Parr, Phys. Rev. B **37**, 785 (1988).

[34] Ch. Lee and C. Sosa, J. Chem. Phys. **100**, 9018 (1994).

[35] (a) R. A. Frosch and K. M. Foley, Phys. Rev. **88**, 1337 (1952); (b) P. Kristiansen and L. Veseth, J. Chem. Phys. **84**, 6336 (1986).

[36] H. Partridge, NASA Technical Memorandum 101044.

[37] P. O. Widmark, P. A. Malmqvist, and B. O. Roos, Theor. Chim. Acta **77**, 291 (1990).

[38] F. B. Van Duijneveldt, IBM Res. J. 945 (#16437) (1971).

[39] D. M. Chipman, Theor. Chim. Acta **76**, 73 (1989); J. Chem. Phys. **91**, 5455 (1989).

[40] S. Huzinaga J. Chem. Phys. **42**, 293 (1965).

[41] S. M. Colwell, C. W. Murray, N. C. Handy, and R. D. Amos, Chem. Phys. Lett. **210**, 261 (1993).

[42] T. H. Dunning, Jr., J. Chem. Phys. **90**, 1007 (1989).

[43] J. Almlöf and P. R. Taylor, Adv. Quantum Chem. **22**, 301 (1991).

[44] W. J. Hehre, R. Ditchfield, and J. A. Pople, J. Chem. Phys. **56**, 2257 (1972).

[45] R. Krishnan, J. S. Binkley, R. Seeger, and J. A. Pople, J. Chem. Phys. **72**, 650 (1980).

[46] T. H. Dunning and P. J. Hay, *Modern Theoretical Chemistry* (Plenum, New York, 1986), pp. 1–28, Chap. 1.

[47] P. Diversi, C. Forte, M. Franceschi, G. Ingrosso, A. Lucherini, M. Petri, and C. Pinzino, J. Chem. Soc. Chem. Commun. 1345 (1992).

[48] E. Hirota and C. Yamada, J. Mol. Spectrosc. **96**, 175 (1985), and references therein.

[49] R. W. Fessenden and R. H. Schuler, J. Chem. Phys. **39**, 2147 (1963).

[50] R. W. Fessenden, J. Phys. Chem. **71**, 74 (1967).

[51] M. T. Rogers and L. D. Kispert, J. Chem. Phys. **46**, 221 (1967).

[52] J. Janecka, H. M. Vyas, and M. Fujimoto, J. Chem. Phys. **54**, 3229 (1971).

[53] T. Shiga, M. Yamaoka, and A. Lund, Z. Naturforsch. Teil A **29**, 653 (1974).

[54] Y. Ellinger, F. Pauzat, V. Barone, J. Douady, and R. Subra J. Chem. Phys. **72**, 6390 (1980).

[55] P. Botschwina, J. Flesch, and W. Meyer, Chem. Phys. **74**, 321 (1983).

[56] D. M. Chipman, J. Chem. Phys. **78**, 3112 (1983).

[57] C. J. Cramer, J. Org. Chem. **16**, 5229 (1991).

[58] J. Pacansky, W. Koch, and M. D. Miller, J. Am. Chem. Soc. **113**, 317 (1991).

[59] V. Tschinke and T. Ziegler, Can. J. Chem. **67**, 480 (1988).

[60] L. Fan and T. Ziegler, J. Chem. Phys. **94**, 6575 (1991).

[61] J. M. Oakes and G. B. Ellison, J. Am. Chem. Soc. **106**, 7734 (1984).

[62] H. J. McManus, R. W. Fessenden, and D. M. Chipman, J. Phys. Chem. **92**, 3778 (1988).

[63] C. L. Currie and D. A. Ramsey, J. Chem. Phys. **45**, 488 (1966).

[64] A. B. Callear and H. K. Lee, Trans. Far. Soc. **64**, 308 (1968).

[65] H. E. van den Bergh and A. B. Callear, Trans. Far. Soc. **66**, 2681 (1970).

[66] N. Nakashima and K. Yoshihara, Laser Chem. **7**, 177 (1987).

[67] G. Maier, H. P. Reisenauer, B. Rohde, and K. Dehnicke, Chem. Ber. **116**, 732 (1983).

[68] A. K. Maltsev, V. A. Korolov, and O. M. Nefdov, Bull. Acad. Sci. USSR, Div. Chem. Sci. **31**, 2131 (1982).

[69] A. K. Maltsev, V. A. Korolov, and O. M. Nefdov, Bull. Acad. Sci. USSR, Div. Chem. Sci. **33**, 510 (1984).

[70] J. W. Huang and W. R. M. Graham, J. Chem. Phys. **93**, 1583 (1990).

[71] J. W. Hudgens and C. S. Dulcey, J. Phys. Chem. **89**, 1505 (1985).

[72] A. D. Snappey and J. C. Weisshaar, J. Phys. Chem. **91**, 3731 (1987).

[73] D. W. Minsek, J. A. Blush, and P. Chen, J. Phys. Chem. **96**, 2025 (1992).

[74] J. A. Blush, D. W. Minsek, J. A. Blush, and P. Chen, J. Phys. Chem. **96**, 10150 (1992).

[75] E. Hirota, C. Yamada, and M. Okunishi, J. Chem. Phys. **97**, 2963 (1992).

[76] E. Hirota, J. Mol. Struct. **320**, 75 (1994).

[77] J. D. Getty, M. J. Burmeister, S. G. Westre, and P. B. Kelly, J. Am. Chem. Soc. **113**, 801 (1991).

[78] J. D. Getty, X. Liu, and P. B. Kelly, J. Phys. Chem. **96**, 10155 (1992).

[79] J. D. Getty and P. B. Kelly, Chem. Phys. **168**, 357 (1992).

[80] J. D. Getty, X. Liu, and P. B. Kelly, Chem. Phys. Lett. 201, 236 (1993).

[81] X. Liu, J. D. Getty, and P. B. Kelly, J. Chem. Phys. **99**, 1522 (1993)

[82] T. Takada and M. Dupuis, J. Am. Chem. Soc. **105**, 1713 (1983).

[83] T. K. Ha, H. Baumann, and J. F. M. Oth, J. Chem. Phys. **85**, 1438 (1986).

[84] C. Cometta-Morini, T. K. Ha, and J. F. M. Oth, J. Mol. Struct. **188**, 79 (1989).

[85] K. Holtzhauer, C. Cometta-Morini, and J. F. M. Oth, J. Phys. Org. Chem. **3**, 219 (1990).

[86] E. Fjogstad and M. YStenes, Spectrochim. Acta Part A **46**, 47 (1990).

[87] P. G. Szalay, A. G. Csazar, G. Fogarasi, A. Karpfen, and H. Lischka, J. Chem. Phys. **93**, 1246 (1990).

[88] F. Sim, D. R. Salahub, S. Chin, and M. Dupuis, J. Chem. Phys. **95**, 4317 (1991).

[89] V. Barone and C. Adamo, Chem. Phys. Lett. **224**, 432 (1994).

[90] V. Barone, Theor. Chim. Acta (to be published).

[91] S. Olivella, Int. J. Quantum Chem. (to be published).

[92] A. Fortunelli and O. Salvetti, Theochem **287**, 89 (1993); A. Fortunelli, Int. J. Quantum Chem. **52**, 97 (1994).

[93] J. P. Perdew and Y. Wang, Phys. Rev. B **33**, 8800 (1986).

[94] Y. Endo, S. Saito, and E. Hirao, J. Chem. Phys. **83**, 2026 (1985).

[95] E. S. Huyser, D. Feller, W. T. Borden, and E. R. Davidson, J. Am. Chem. Soc. **104**, 2956 (1982).

[96] S. Kuroda and I. Miyagawa, J. Chem. Phys. **76**, 3933 (1982).